Frictional Resistance of Antifouling Coating Systems

Michael P. Schultz
Department of Naval Architecture and Ocean Engineering,
United States Naval Academy,
Annapolis, MD 21402

An experimental study has been made to compare the frictional resistance of several ship hull coatings in the unfouled, fouled, and cleaned conditions. Hydrodynamic tests were completed in a towing tank using a flat plate test fixture towed at a Reynolds number (Re_L) range of $2.8\times10^6-5.5\times10^6$ based on the plate length and towing velocity. The results indicate little difference in frictional resistance coefficient (C_F) among the coatings in the unfouled condition. Significant differences were observed after 287 days of marine exposure, with the silicone antifouling coatings showing the largest increases in C_F. While several of the surfaces returned to near their unfouled resistance after cleaning, coating damage led to significant increases in C_F for other coatings. The roughness function ΔU^+ for the unfouled coatings showed reasonable collapse to a Colebrook-type roughness function when the centerline average height ($k=0.17R_a$) was used as the roughness length scale. Excellent collapse of the roughness function for the barnacle fouled surfaces was obtained using a new roughness length scale based on the barnacle height and percent coverage. [DOI: 10.1115/1.1845552]

Introduction

The settlement and subsequent growth of flora and fauna on surfaces exposed in aquatic environments is termed biofouling. Biofouling on ship hulls leads to increased surface roughness, frictional resistance, and fuel consumption, e.g. [1–6]. A recent paper by Townsin [7] provides a comprehensive review of much of the research in this area. In order to control the problem, antifouling (AF) coatings are used. Most of these coatings incorporate biocides which are toxic to marine organisms. The environmental impact of tributyl tin (TBT) biocides in AF coatings has led to their ban on vessels of length <25 m in most industrialized countries [8], and a worldwide ban on the application of TBT AF coatings on all vessels was imposed by the International Maritime Organization in 2003 [9]. Copper-based coatings are the primary replacement for TBT coatings, but they are less effective in controlling fouling and may also become the target of environmental legislation. For this reason, there has been a great deal of interest in developing non-toxic replacements, e.g., [10,11]. The most promising alternatives to date are polydimethylsiloxane (PDMS) silicone elastomer coatings [12,13]. These coatings, termed fouling release, do not prevent fouling settlement [14] but reduce the adhesion strength of the fouling organisms by an order of magnitude or more compared to traditional AF coatings [15]. Since fouling-release coatings do not prevent fouling, they must be easily cleaned mechanically or be self-cleaning at operational speeds in order to be effective [16].

The effect of hull condition is of great importance to the performance of marine vehicles. Skin friction on some hull types can account for as much as 90% of the total drag even when the hull is free of fouling [17]. For this reason, understanding and predicting frictional drag has been the focus of a substantial body of research. Several previous investigations have looked at the effect of surface roughness on the frictional drag of unfouled marine paints. These include studies by Musker [18], Townsin et al. [19], Granville [20], Medhurst [21], and Grigson [22]. Most of this work centered on characterizing the change in roughness and drag of the self polishing copolymer (SPC) TBT systems. No effort to address the effect of fouling was made. This was likely due to the fact that the TBT systems provided long term fouling control with minimal fouling settlement.

A great deal of research has also been devoted to studying the effects of fouling on drag. Much of this has addressed calcareous macrofouling (e.g., barnacles, oysters, etc.) and is reviewed in *Marine Fouling and Its Prevention* [23]. Similar studies focusing on the effect of plant fouling and biofilms date back to McEntee [24]. Further work to better quantify the effect that slime films have on drag was carried out by Benson et al. [2], Denny [3], Watanabe et al. [5], and Picologlou et al. [25]. More recently, Lewthwaite et al. [4] and Haslbeck and Bohlander [26] conducted full-scale ship tests to determine the effect of fouling on the drag of copper-based coatings. Schultz and Swain [27] and Schultz [28] used laser Doppler velocimetry to study the details of turbulent boundary layers developing over biofilms and filamentous algae, respectively. The results of all these studies indicate that relatively thin fouling layers can significantly increase drag.

Despite the fairly large body of research that has been conducted, there are little if any reliable data available to compare the hydrodynamic performance of the nontoxic, fouling-release surfaces with the biocide-based systems over the coating life cycle. Some preliminary data from Candries et al. [11] seem to indicate that in the unfouled condition, fouling-release systems may have slightly less frictional resistance than traditional AF coatings despite having a larger mean roughness. These results have yet to be validated and no data were offered for fouled coatings or for fouled coatings that have been cleaned. The purpose of the present research is to compare the performance of fouling-release coatings with biocide-based AF coatings in the unfouled, fouled, and cleaned conditions.

Background

The mean velocity profile in the inner portion of a turbulent boundary layer, outside of the viscous sublayer, can be expressed as the classical log law

$$U^+=\frac{1}{\kappa}\ln(y^+)+B. \tag{1}$$

Clauser [29] contended that the mean velocity profile in the inner layer of rough wall flows also exhibits a log law with the same slope as that of the smooth wall outside the roughness sublayer. The log-law intercept, however, is shifted downward from that of

Contributed by the Fluids Engineering Division for publication in the JOURNAL OF FLUIDS ENGINEERING. Manuscript received by the Fluids Engineering Division March 21, 2004; revised manuscript received June 12, 2004. Review conducted by: Steven L. Ceccio.

Report Documentation Page

Form Approved
OMB No. 0704-0188

1. REPORT DATE	2. REPORT TYPE	3. DATES COVERED
JUN 2004		**00-00-2004 to 00-00-2004**

4. TITLE AND SUBTITLE	5a. CONTRACT NUMBER
Frictional Resistance of Antifouling Coating Systems	5b. GRANT NUMBER
	5c. PROGRAM ELEMENT NUMBER
6. AUTHOR(S)	5d. PROJECT NUMBER
	5e. TASK NUMBER
	5f. WORK UNIT NUMBER
7. PERFORMING ORGANIZATION NAME(S) AND ADDRESS(ES) **United States Naval Academy,Department of Naval Architecture and Ocean Engineering,Annapolis,MD,21402**	8. PERFORMING ORGANIZATION REPORT NUMBER
9. SPONSORING/MONITORING AGENCY NAME(S) AND ADDRESS(ES)	10. SPONSOR/MONITOR'S ACRONYM(S)
	11. SPONSOR/MONITOR'S REPORT NUMBER(S)

12. DISTRIBUTION/AVAILABILITY STATEMENT
Approved for public release; distribution unlimited

13. SUPPLEMENTARY NOTES

14. ABSTRACT

15. SUBJECT TERMS

16. SECURITY CLASSIFICATION OF:			17. LIMITATION OF ABSTRACT	18. NUMBER OF PAGES	19a. NAME OF RESPONSIBLE PERSON
a. REPORT	b. ABSTRACT	c. THIS PAGE			
unclassified	**unclassified**	**unclassified**	**Same as Report (SAR)**	**9**	

the smooth wall. The downward shift is called the roughness function ΔU^+, and can be used to express the log law over rough walls as follows:

$$U^+ = \frac{1}{\kappa}\ln(y^+) + B - \Delta U^+. \tag{2}$$

ΔU^+ is a function of the roughness Reynolds number k^+ defined as the ratio of the roughness length scale k to the viscous length scale ν/U_τ.

Clauser [29] and Hama [30] both proposed that the outer region of the boundary layer for both smooth and rough walls obeys the velocity defect law given as

$$\frac{U_e - U}{U_\tau} = f\left(\frac{y}{\delta}\right). \tag{3}$$

The physical implication of a universal defect law is that the mean velocity in the outer layer is independent of surface condition except for the effect that it has on U_τ. Experimental support for a universal velocity defect profile on smooth and rough walls can be found in recent studies by Krogstad and Antonia [31] and Schultz and Flack [32]. Hama [30] showed that by evaluating Eqs. (1)–(3) for $y = \delta$ at the same value of the displacement thickness Reynolds number Re_{δ^*}, the roughness function can be expressed as

$$\Delta U^+ = \left(\sqrt{\frac{2}{c_f}}\right)_S - \left(\sqrt{\frac{2}{c_f}}\right)_R. \tag{4}$$

Granville [20] offers an alternative method for determining the roughness function indirectly. In this method, the overall frictional drag of a flat plate covered with a given roughness is related to the local wall shear stress and mean velocity profile at the trailing edge of the plate. The analysis is based on the assumption of boundary layer similarity for rough and smooth walls as expressed in Eqs. (1)–(3). Granville's procedure involves comparing the C_F values of smooth and rough plates at the same value of $\mathrm{Re}_L C_F$. The resulting equations for k^+ and ΔU^+ are given in Eqs. (5) and (6), respectively.

$$k^+ = \left(\frac{k}{L}\right)\left(\frac{\mathrm{Re}_L C_F}{2}\right)\left(\sqrt{\frac{2}{C_F}}\right)_R\left[1 - \frac{1}{\kappa}\left(\sqrt{\frac{C_F}{2}}\right)_R + \frac{1}{\kappa}\left(\frac{3}{2\kappa} - \Delta U^{+\prime}\right)\left(\frac{C_F}{2}\right)_R\right] \tag{5}$$

$$\Delta U^+ = \left(\sqrt{\frac{2}{C_F}}\right)_S - \left(\sqrt{\frac{2}{C_F}}\right)_R - 19.7\left[\left(\sqrt{\frac{C_F}{2}}\right)_S - \left(\sqrt{\frac{C_F}{2}}\right)_R\right] - \frac{1}{\kappa}\Delta U^{+\prime}\left(\sqrt{\frac{C_F}{2}}\right)_R \tag{6}$$

Further details of the development of these equations are given in [20]. Recent results by Schultz and Myers [33] show good agreement between the roughness functions determined by Granville's method and those measured directly using the local mean velocity profile. It is of note that once $\Delta U^+ = f(k^+)$ for a roughness, it can be used in a computational boundary layer code or a similarity law analysis [34] to predict the drag of any body covered with that roughness.

Experimental Facilities and Method

The experiments were conducted in the 115 m long towing tank facility at the United States Naval Academy Hydromechanics Laboratory, Annapolis, Maryland. The experimental facilities and method used in the present study were similar to those used by Schultz [35]. The width and depth of the tank are 7.9 m and 4.9 m, respectively. The towing carriage has a velocity range of 0–7.6 m/s. In the present study, the towing velocity was varied between 2.0 and 3.8 m/s ($\mathrm{Re}_L = 2.8\times10^6 - 5.5\times10^6$). The velocity of the towing carriage was measured and controlled using an encoder on the rails that produce 4000 pulses/m. Using this system, the precision uncertainty in the mean velocity measurement was $<0.02\%$ over the entire velocity range tested. The working fluid in the

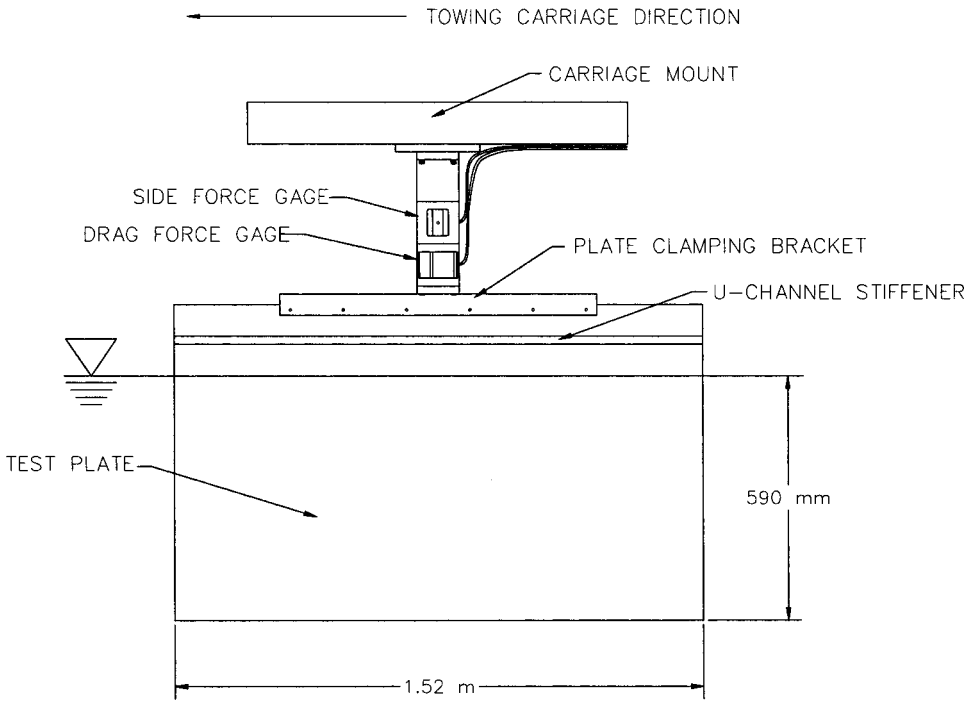

Fig. 1 Schematic of the flat plate test fixture

Table 1 Fouling coverage for the AF surfaces after 287 days exposure. Results are expressed in accordance with ASTM D3623 [36].

Test surface	Total fouling coverage (%)	Slime (%)	Hydroids (%)	Barnacles (%)	Fouling description
Silicone 1	75	10	5	60	Uniform coverage of barnacles (~6 mm in height)
Silicone 2	95	15	5	75	Uniform coverage of barnacles (~7 mm in height)
Ablative copper	76	75	0	1	Dense layer of diatomaceous and bacterial slime with very isolated barnacles (~5 mm in height)
SPC copper	73	65	3	4	Moderate layer of diatomaceous and bacterial slime with isolated barnacles (~5 mm in height)
SPC TBT	70	70	0	0	Light layer of diatomaceous and bacterial slime (~1 mm in height)

experiments was fresh water, and the temperature was monitored to within ± 0.05°C during the course of the experiments using a thermocouple with digital readout.

Figure 1 shows a schematic of the test fixture and plate. The flat test plate was fabricated from 304 stainless steel sheet stock and measured 1.52 m in length, 0.76 m in width, and 3.2 mm in thickness. Both the leading and trailing edges were filleted to a radius of 1.6 mm. No tripping device was used to stimulate transition. The overall drag of the plate was measured using a Model HI-M-2, modular variable-reluctance displacement force transducer manufactured by Hydronautics Inc. An identical force transducer, rotated 90° to the drag gauge, was included in the test rig to measure the side force on the plate. The purpose of the side force gage was to ensure precise alignment of the plate. This was accomplished by repeatedly towing the plate at a constant velocity and adjusting the yaw angle of the test fixture to minimize the side force. Once this was done, no further adjustments were made to the alignment over the course of the experiments. The side force was monitored throughout to confirm that the plate alignment did not vary between test surfaces. Both of the force transducers used in the experiments had load ranges of 0–110 N. The combined bias uncertainty of the gages is $\pm 0.25\%$ of full scale. Data were gathered at a sampling rate of 100 Hz and were digitized using a 16-bit analog-to-digital converter. The sampling duration ranged from 30 s per test run at the lowest Reynolds number to 10 s per test run at the highest Reynolds number. The overall drag was first measured with 590 mm of the plate submerged. This was repeated with 25 mm of the plate submerged in order to find the wavemaking resistance tare. The difference between the two was taken to be the frictional resistance on the two 565 mm wide by 1.52 m long faces of the plate. The tests were repeated three times for each surface and Reynolds number. The results presented are the means of these runs.

Five antifouling coating systems were tested. Two of these were PDMS silicone AF systems, which will be referred to as silicone 1 and 2. One was an ablative copper AF system, typical of that presently used by the U.S. Navy on its surface combatants. SPC copper and SPC TBT paint systems were also tested. All of the paints were applied as directed by the paint manufacturer using the suggested surface preparation, primer, and tiecoat. The paint application was carried out by the Naval Surface Warfare Center-Carderock, Paints and Processes Branch (Code 641) using airless spray. Three control surfaces were also tested. These included test plates covered with 60-grit and 220-grit wet/dry sandpaper and a polished smooth surface. The surface profiles of all the test plates before exposure in the marine environment and after cleaning were measured using a Cyber Optics laser diode point range sensor laser profilometer system mounted to a Parker Daedal two-axis traverse with a resolution of 5 μm. The resolution of the sensor is 1 μm with a laser spot diameter of 10 μm. Data were taken over a sampling length of 50 mm and were digitized at a sampling interval of 25 μm. Ten linear profiles were taken on each of the test surfaces. A single three-dimensional topographic profile was made on each of the surfaces by sampling over a square area 2.5 mm on a side with a sampling interval of 25 μm.

The antifouling coatings were tested in three different conditions; unfouled, fouled, and cleaned. The unfouled condition was the as-applied painted surface, prior to marine exposure. The fouled condition was after exposure in the Severn River (Annapolis, Maryland) from September 16, 2002 until June 30, 2003 (287 days). The cleaned condition was the test surface after removal of the fouling using a nylon brush. It should be noted that the control test surfaces were not exposed in the marine environment. The exposure site at the U.S. Naval Academy was located near the confluence of the Severn River and the Chesapeake Bay (Annapolis, Maryland). The test plates were held vertically at ~0.2 m

Table 2 Roughness statistics for all test surfaces in the unfouled and cleaned condition

	Unfouled			Cleaned		
Test surface	R_a (μm)	R_q (μm)	R_t (μm)	R_a (μm)	R_q (μm)	R_t (μm)
Silicone 1	12±2	14±2	66±7	10±2	13±2	76±11
Silicone 2	14±2	17±2	85±8	19±1	23±1	142±21
Ablative copper	13±1	16±1	83±6	11±1	14±1	77± 5
SPC copper	15±1	18±1	97±10	18±2	23±2	112± 5
SPC TBT	20±1	24±2	129±9	22±2	27±2	135± 7
60-grit SP	126±5	160±7	983±89	NA	NA	NA
220-grit SP	30±2	38±2	275±17	NA	NA	NA
Smooth	<1	<1	<1	NA	NA	NA

Note: Uncertainties represent 95% confidence precision error bounds.

below the mean low water level. The plates were exposed and the fouling coverage was evaluated according to ASTM D3623 [36]. The water temperature at the exposure site ranged from 1°C to 27°C and the salinity from 4 ppt to 10 ppt during the exposure period. The fouling coverage after 287 days is given in Table 1. After hydrodynamic testing, the fouled plates were cleaned using a nylon brush and a garden hose. The surface roughness of the test surfaces in the unfouled and cleaned condition is given in Table 2.

Uncertainty Estimates

Precision uncertainty estimates for the frictional drag measurements were made through repeatability tests using the standard procedure outlined by Moffat [37]. Three replicate towing tests were made with each surface at each Reynolds number. The standard error for C_F was then calculated. The 95% precision confidence limits for a mean statistic were obtained by multiplying the standard error by the two-tailed t value ($t=4.303$) for two degrees of freedom given by Coleman and Steele [38]. The resulting precision uncertainties in C_F were $\leqslant \pm 1\%$ for all the tests. The overall precision and bias error was dominated by the systematic error due to the combined bias of the force gages ($\pm 0.25\%$ of full scale). The resulting precision and bias uncertainty in C_F ranged from $\pm 5\%$ at the lowest Reynolds number to $\pm 2\%$ at the highest Reynolds number. To insure the accuracy of the results, the control sandpaper and smooth test plates were run periodically throughout the experiments to check that the resulting mean C_F value was within the precision uncertainty bounds that had previously been obtained. The overall precision and bias error for the roughness function ΔU^+ ranged from $\pm 16\%$ or 0.2 (whichever is larger) at the lowest Reynolds number to $\pm 6\%$ or 0.1 (whichever is larger) at the highest Reynolds number.

Results and Discussion

The presentation of the results and discussion will be organized as follows. First, the frictional resistance results will be presented for the test surfaces in the unfouled, fouled, and cleaned conditions. These results will then be used to develop a relationship between the physical surface roughness and the roughness function ΔU^+. Finally, the frictional resistance will be scaled up to ship scale using similarity law analysis to determine the likely effect of these forms of roughness on ship frictional resistance.

Frictional Resistance, C_F. The results of the frictional resistance tests for the surfaces in the unfouled condition are presented in Fig. 2. The Kármán-Schoenherr friction line for a smooth plate is also shown for comparison [39]. This friction line is defined as

$$\frac{0.242}{\sqrt{C_F}} = \log(\mathrm{Re}_L C_F). \tag{7}$$

The present smooth plate results agree within ~1% with the Kármán-Schoenherr friction line as was also observed in a previous investigation in this facility [35]. At the lowest Reynolds number, the AF test surfaces all showed an increase in C_F compared to the smooth control. Silicone 1 and 2 had the smallest increase (1%), while the SPC TBT surface had the largest one (4%). It should be noted that while all of the AF surfaces had higher frictional resistance at the lowest Reynolds number than the smooth control, the differences were within the experimental uncertainty of the measurements. The 60-grit and 220-grit sandpaper controls exhibited increases in C_F of 66% and 17%, respectively, compared to the smooth test surface at the lowest Reynolds number. The effect of the surface roughness became larger with increasing Reynolds number. The increase in C_F for the AF surfaces ranged from 4% for silicone 1 to 8% for the SPC TBT surface at the highest Reynolds number. These differences are beyond the combined experimental uncertainty of the measurements and can be considered significant. The 60-grit and 220-grit sandpaper controls had increases in C_F of 83% and 31%, respectively, at the highest Reynolds number. Although the silicone fouling-release surfaces tended to have lower frictional resistance than the other AF surfaces over the entire range of Reynolds number tested, the differences observed were within the experimental uncertainty. A trend of lower drag on silicone fouling-release surfaces than for traditional AF paints was also noted by Candries et al. [11]. In the present case, the lower drag can be explained by the fact that the silicone surfaces were smoother than the other AF surfaces (Table 2). However, Candries et al. [11,40] noted lower drag even when the silicones were rougher than traditional AF surfaces. They attributed the lower drag to the longer wavelength of the roughness inherent for silicone coatings. Figure 3 shows representative surface profiles for Silicone 1 and the ablative copper coating that illustrate the differences in the roughness between silicones and traditional biocide-based AF coatings. It can be seen that the silicone roughness is populated by longer wavelengths than the copper surface. The wave-number spectra for the two surfaces presented in Fig. 4 clearly show a greater contribution to the roughness from the low wave-number scales on the silicone as compared to the copper surface. The relationship between the surface roughness and the increase in drag will be discussed further in the roughness function section.

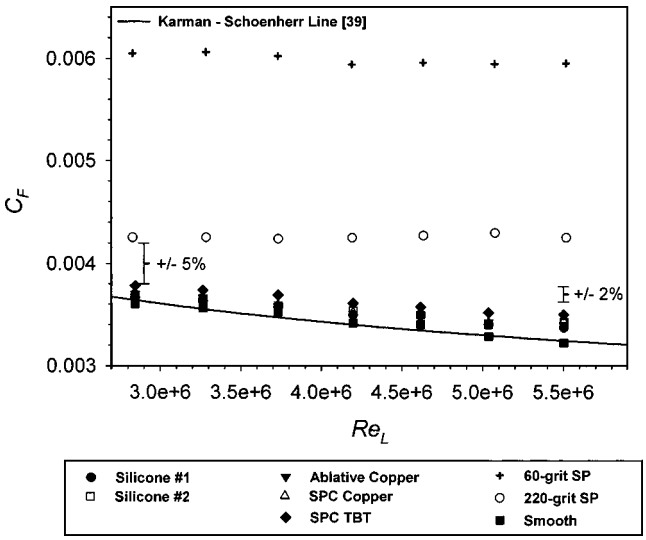

Fig. 2 Overall frictional resistance coefficient versus Reynolds number for all test surfaces in the unfouled condition. (Overall uncertainty in C_F: ±2% at highest Reynolds number; ±5% at lowest Reynolds number.)

The results of the frictional resistance tests for the surfaces in the fouled condition are presented in Fig. 5. All of the fouled surfaces exhibited a significant increase in frictional resistance compared to the smooth control over the entire Reynolds number range. The increase was greatest for the two silicone plates, which had C_F values three to four times higher than the smooth surface. These surfaces, not surprisingly, had the heaviest coverage of barnacles. These results indicate that if silicones are to be effective ship hull coatings they must be capable of hydrodynamic self-cleaning or be easily cleaned mechanically. The towing speeds in the present study were not high enough to cause significant self-cleaning of the coating. Further studies are needed in which the coated surfaces are towed at higher speeds in order to address the possible effect of self-cleaning on the drag. The ablative copper and SPC copper surfaces, which showed much lighter barnacle fouling (1%–4%), had increases in C_F that ranged from 87%–138%. The present results support findings of the classic pontoon resistance experiments carried out by Kempf [1] which also showed very large increases in frictional resistance with barnacle fouling. Recently, similar results were obtained in uncoated pipe flow experiments over barnacles by Leer-Andersen and Larsson

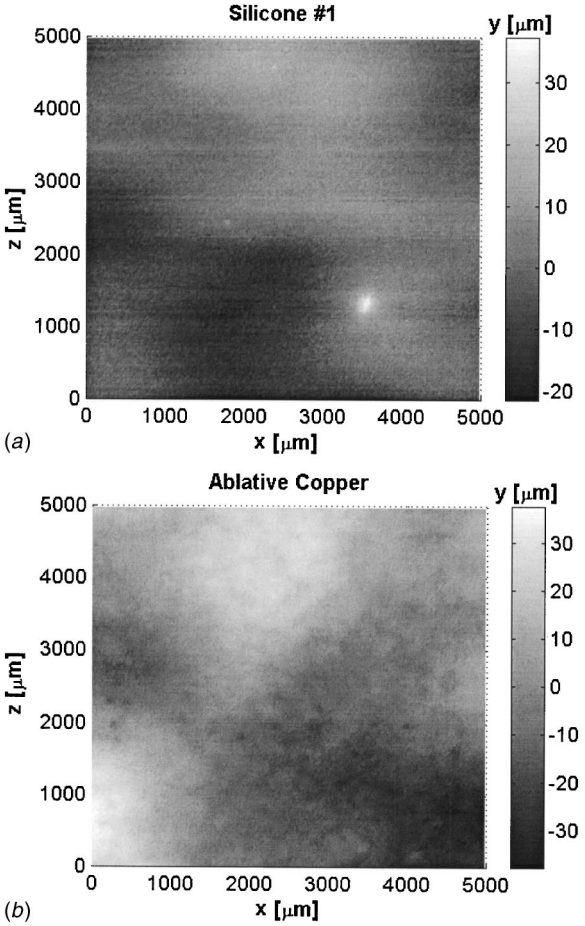

Fig. 3 Plan view of the surface waveform for (a) silicone 1 specimen; (b) Ablative copper specimen. (Overall uncertainty: *y* direction, ±1 μm; *x* and *z* directions, ±5 μm.)

[6]. It is of note that the SPC TBT surface showed an increase in C_F of 58%–68%, despite being covered with only a thin layer of slime. This supports the observations of Schultz and Swain [27] and Haslbeck and Bohlander [26] that show that surfaces covered with a light biofilm, otherwise free of calcareous fouling, can exhibit a significant increase in drag. The relationship between the fouling coverage and the increase in drag will be discussed further in the roughness function section. It should be noted that the present drag tests were carried out in fresh water, not the estuarine water that the fouling developed in. However, there was little difference visually in the fouling before and after exposure to the fresh water, and the invertebrate organisms, such as barnacles, remained alive. Also, since the salinity of the estuarine water was low, it is not felt that testing in fresh water caused undue stress on the fouling or significantly affected the results.

The results of the frictional resistance tests for the surfaces in the cleaned condition are presented in Fig. 6. All the AF surfaces showed an increased C_F as compared to the smooth control at the lowest Reynolds number. Silicone 1 and the ablative copper showed the smallest increase (3%), while the SPC TBT surface had the largest drag increment (7%). However, these differences were within the experimental uncertainty of the measurements. The effect of the surface roughness was more pronounced at

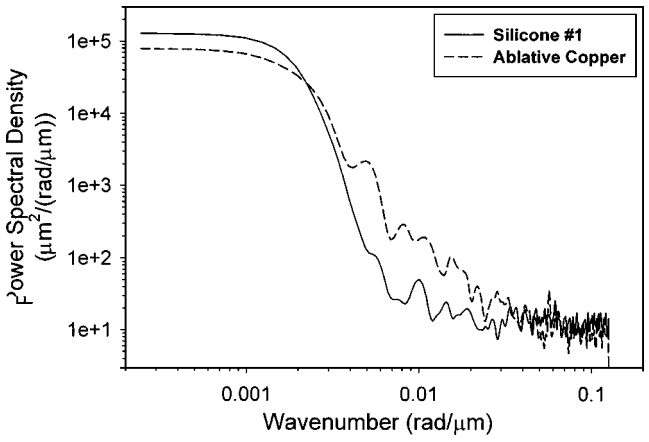

Fig. 4 Wave-number spectra of the surface waveforms for silicone 1 and ablative copper

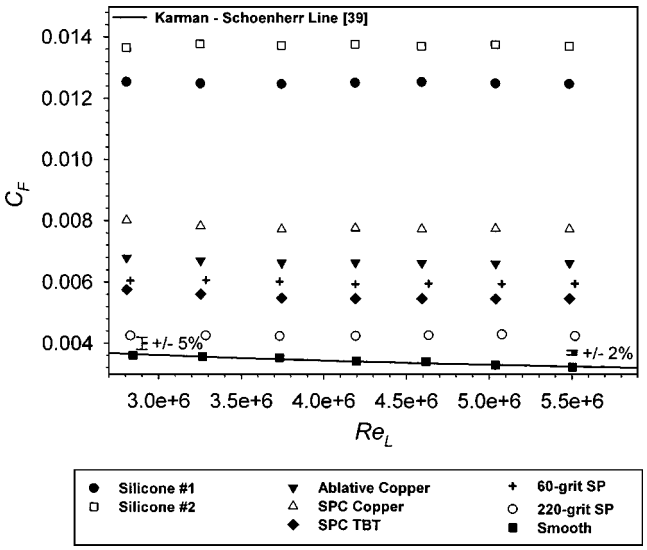

Fig. 5 Overall frictional resistance coefficient versus Reynolds number for all test surfaces in the fouled condition after 287 days exposure. (Overall uncertainty in C_F: ±2% at highest Reynolds number; ±5% at lowest Reynolds number.)

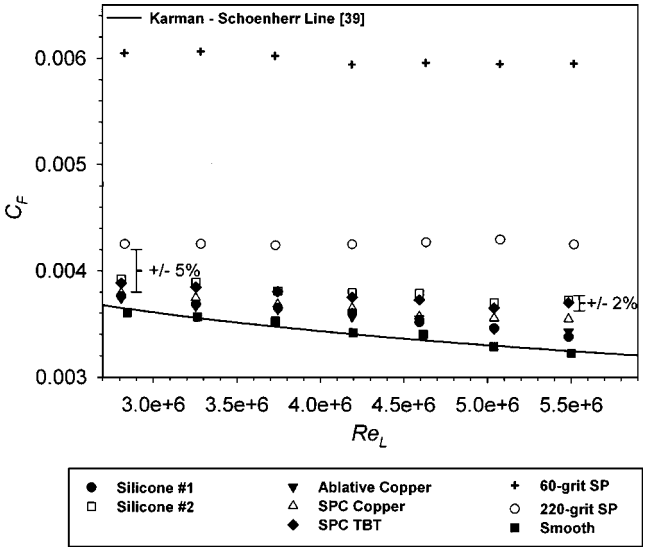

Fig. 6 Overall frictional resistance coefficient versus Reynolds number for all test surfaces in the cleaned condition. (Overall uncertainty in C_F: ±2% at highest Reynolds number; ±5% at lowest Reynolds number.)

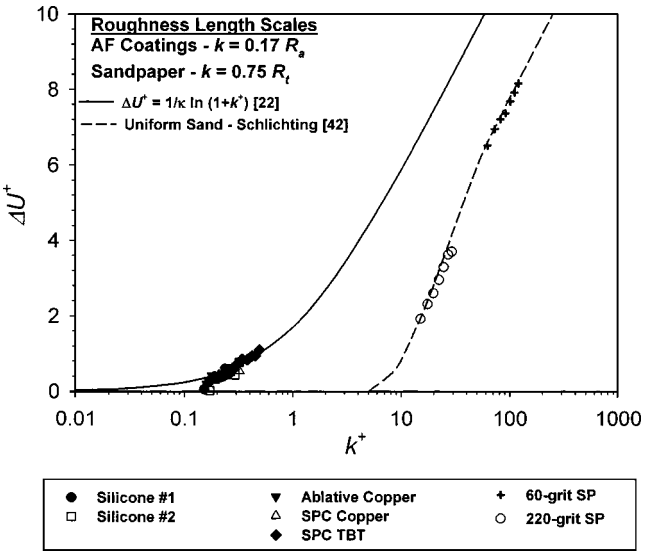

Fig. 7 Roughness function for all test surfaces in the unfouled condition. [Overall uncertainty in ΔU^+: ±6% or ±0.1 (whichever is larger) at highest Reynolds number; ±16% or ±0.2 (whichever is larger) at lowest Reynolds number.]

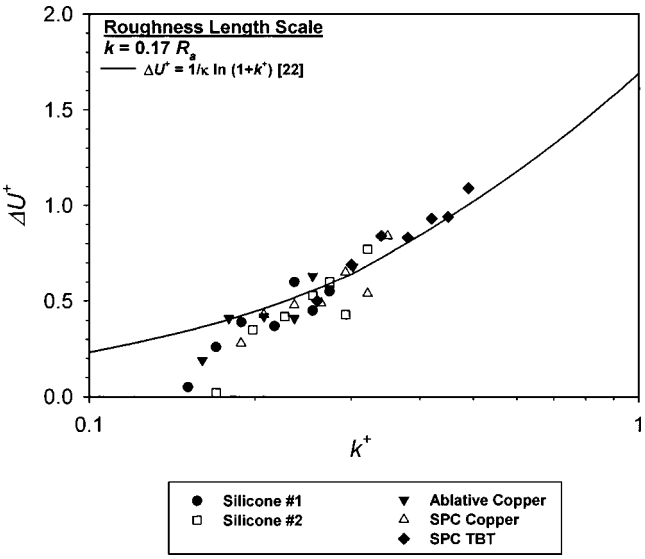

Fig. 8 Roughness function for the AF test surfaces in the unfouled condition. [Overall uncertainty in ΔU^+: ±6% or ±0.1 (whichever is larger) at highest Reynolds number; ±16% or ±0.2 (whichever is larger) at lowest Reynolds number.]

higher Reynolds number. The increase in C_F for the AF surfaces ranged from 5% for silicone 1 to 15% for silicone 2 compared to the smooth control at the highest Reynolds number. These differences are greater than the combined experimental uncertainty of the measurements and are considered significant. The ablative copper and silicone 1 both returned to nearly their unfouled frictional resistance, while silicone 2 and the SPC TBT showed significant increases in resistance. The roughness on the ablative copper, silicone 1, and the SPC TBT did not change from the unfouled to the cleaned conditions (Table 2), while the roughness on silicone 2 increased. It is believed that isolated coating damage due to exposure and cleaning led to increased drag on the SPC TBT surface, although it was isolated enough not to significantly affect the measured roughness statistics. The differences in surface roughness and how they relate to the frictional resistance will be discussed further in the roughness function section.

Roughness Function ΔU^+. The roughness functions ΔU^+ for the test surfaces in the unfouled, fouled, and cleaned condition were found by means of the similarity law analysis of Granville [20] developed for flat plates. This was carried out by solving Eqs. (5) and (6) iteratively for k^+ and ΔU^+, respectively. It should be noted that the choice of k for a given roughness has no effect on the calculated ΔU^+ despite its apparent dependence on k through the $\Delta U^{+\prime}$ term in Eqs. (5) and (6). This is because the effect of changing k on ΔU^+ is to simply move the curve along the abscissa without changing its slope. The roughness function results for all the test surfaces in the unfouled condition are shown in Fig. 7 and for the unfouled AF surfaces in Fig. 8. Shown for comparison is the roughness function for uniform sand given by Schlichting [41] based on the classical experiments of Nikuradse [42] and a Colebrook-type roughness function of Grigson [22] for random roughness given as

$$\Delta U^+ = \frac{1}{\kappa}\ln(1+k^+). \tag{8}$$

The roughness functions for the rough sandpaper controls show excellent agreement with a Schlichting uniform sand roughness function using $k=0.75R_t$. This was also observed in previous investigations by the present author using a range of direct and indirect methods to obtain ΔU^+ [32,33]. All of the roughness length scales in Table 2, as well as moments of the wavenumber spectra (i.e., Townsin et al. [19]), the mean absolute roughness slope (i.e., Musker [18]) and combinations thereof, were considered as possible roughness length scales for the unfouled AF surfaces. The best fit of these results was found using a simple multiple of the centerline average height, R_a, as k. R_a was suggested to be a suitable roughness scaling parameter for sanded paint surfaces by Schultz and Flack [32]. With $k=0.17R_a$, 75% of the variance (i.e., $R^2=0.75$) in ΔU^+ could be explained using a Colebrook-type roughness function [Eq. (8)]. The results presented in Figs. 7 and 8 show that reasonable agreement is obtained using this scaling considering the relatively large uncertainty in ΔU^+ as $k^+\rightarrow 0$. Candries et al. [40] assert that a roughness parameter based on both R_a and the mean absolute slope adequately collapses a range of unfouled AF surfaces. This scaling was tried in the present study, but did no better job of collapsing the results than R_a alone. It is of note that the scatter in ΔU^+ in the study of Candries et al. was larger than in the present study. The results seem to indicate that the differences in roughness wavelength observed between the silicones and traditional AF paints in this study (see Figs. 3 and 4) are not large enough to significantly influence the frictional drag.

The roughness functions for the fouled surfaces are presented in Fig. 9. In order to develop suitable scaling parameters for the fouled surfaces it was decided to divide the surfaces into those with barnacle fouling and those without (only the SPC TBT surface). In developing a scaling parameter for the surfaces with barnacle fouling, it was assumed that the largest roughness heights (i.e., the height of the largest barnacles) have the dominant influence on drag and that effect of increased percent coverage of barnacles on drag is largest for small coverage and smaller for large coverage. These assumptions were gleaned from the present results and the pipe flow experiments of Leer-Andersen and Larsson [6], as well as the observations of Bradshaw for typical roughness types [43]. Based on this, the following roughness length scale was developed for the barnacle-fouled surfaces:

$$k=0.059R_t(\%\ \text{Barnacle Fouling})^{1/2}. \tag{9}$$

R_t here is taken to be the height of the largest barnacles, given in the last column of Table 1. Using this scaling, excellent collapse ($R^2=0.98$) is obtained for the present results with a Colebrook-type roughness function [Eq. (8)]. Further study is needed to assess the validity of this scaling on a range of fouled surfaces and

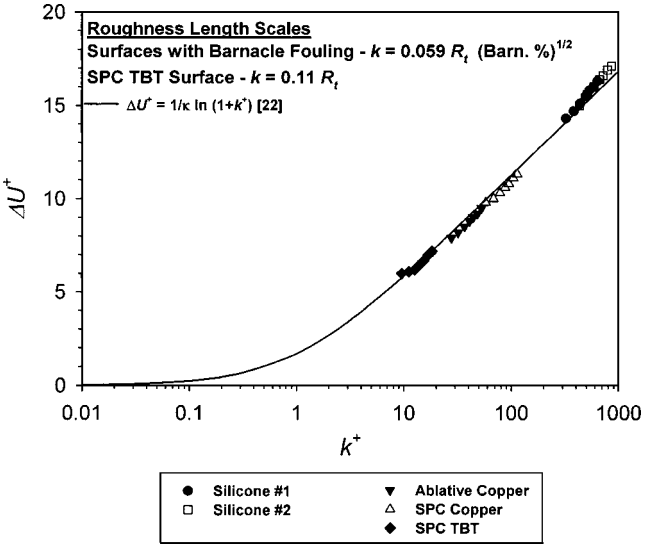

Fig. 9 Roughness function for the AF test surfaces in the fouled condition after 287 days exposure. [Overall uncertainty in ΔU^+: ±6% or ±0.1 (whichever is larger) at highest Reynolds number; ±16% or ±0.2 (whichever is larger) at lowest Reynolds number.]

its applicability to other calcareous fouling types. The SPC TBT remained free of barnacle fouling over the course of exposure and was covered with only a light slime film. The roughness function for this surface collapsed well ($R^2=0.90$) with a Colebrook-type roughness function [Eq. (8)] using $k=0.11R_t$, where R_t is the estimated thickness of the slime film using a wet film paint thickness gauge, given in the last column of Table 1. The slime film thickness measurement procedure is described in greater detail in Schultz and Swain [27].

The roughness functions for the cleaned surfaces are presented in Fig. 10. It was decided to use the same roughness scaling for the cleaned AF surfaces as for the unfouled surfaces ($k=0.17R_a$). As can be seen in Fig. 10, this choice of k gives poor collapse of the results. Other choices did not yield significant

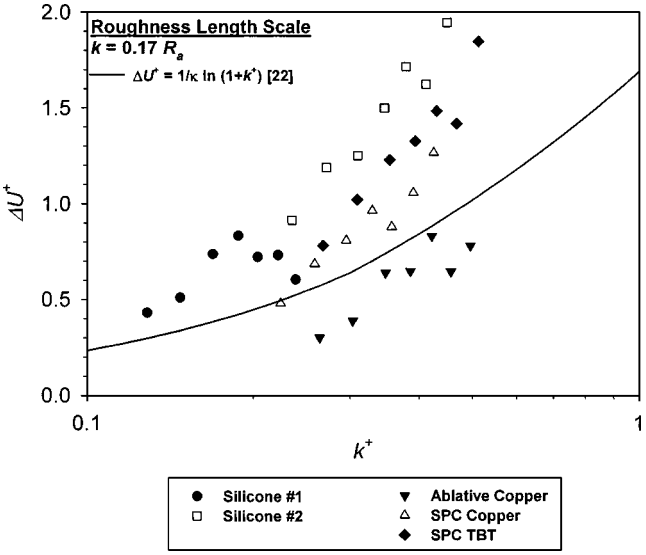

Fig. 10 Roughness function for the AF test surfaces in the cleaned condition. [Overall uncertainty in ΔU^+: ±6% or ±0.1 (whichever is larger) at highest Reynolds number; ±16% or ±0.2 (whichever is larger) at lowest Reynolds number.]

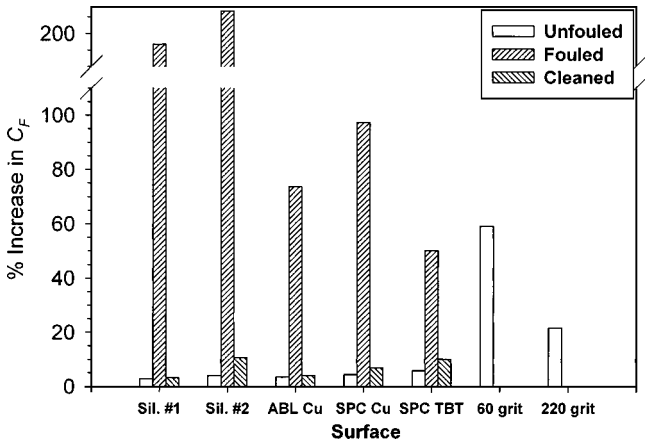

Fig. 11 Increase in C_F at ship-scale ($L=150$ m) for the test surfaces in the unfouled, fouled, and cleaned conditions for $U\approx 6.2$ m/s (12 knots)

improvement. It is felt that the inability to collapse results for the cleaned surfaces stems from small areas of coating damage due to exposure in the marine environment and subsequent cleaning. The likelihood of these areas being randomly sampled when the roughness height measurements are made is small. However, the effect of the damage on the overall frictional resistance of the surface is quite significant. Further work is, therefore, needed to identify a robust roughness scaling parameter and sampling routine suitable for a wider range of coating types and conditions.

Frictional Resistance, C_F, at Ship-Scale. Granville [34] gives a similarity law procedure for calculating the effect of a given roughness on the frictional resistance of a planar surface of arbitrary length using the roughness function obtained for a flat plate in a lab. This was carried out using the present highest Reynolds number results for a plate length, L, of 150 m. This length was selected because it is representative of many midsized merchant ships as well as Naval surface combatants such as frigates and destroyers. Figure 11 shows the results of the similarity law analysis for all surfaces in the unfouled, fouled, and cleaned conditions for $U\approx 6.2$ m/s (12 knots). The results are presented as percent increase in C_F compared to a smooth surface. The increase in C_F for the AF surfaces in the unfouled condition ranged from 3% for silicone 1 to 6% for the SPC TBT surface. This indicates that only small differences in the performance of these coatings are likely when a ship is freshly out of drydock. The 60-grit and 220-grit sandpaper controls had increases in C_F of 59% and 22%, respectively.

The increase in C_F for the AF surfaces in the fouled condition ranged from 50% for SPC TBT to 217% for the silicone 2. The two silicone surfaces had the largest increase in frictional resistance with the biocide-based AF systems showing smaller increase. This indicates that silicones will likely provide significantly poorer performance than biocide-based systems if hydrodynamic self-cleaning is not possible or if mechanical cleaning is not utilized. The increase in C_F for the AF surfaces in the cleaned condition ranged from 3% for silicone 1 to 11% for silicone 2. It is of note that the frictional resistance for silicone 1, ablative copper, and SPC copper returned to within 1% of the unfouled condition, while silicone 2 and SPC TBT had increases of 7% and 4%, respectively, compared to the unfouled resistance. This difference is likely due to small areas of coating damage that were discussed previously.

Conclusion

An experimental study of the surface roughness and frictional resistance of a range of modern antifouling paint systems has been

made. The results indicate little difference in C_F among the paint systems in the unfouled condition. Significant differences, however, were observed in C_F among the paint systems in the fouled condition, with the silicone surfaces showing the largest increases. While some of the antifouling systems returned to near their unfouled resistance after cleaning, coating damage led to significant increases in C_F for some coatings. The roughness function ΔU^+ for the unfouled coatings shows reasonable collapse to a Colebrook-type roughness function when the centerline average height ($k=0.17R_a$) is used as the roughness length scale. Excellent collapse of the roughness function for the barnacle fouled surfaces was obtained using a new roughness length scale based on the barnacle height and percent coverage. Poor collapse of the roughness function for the cleaned coatings was likely due to isolated damage.

Acknowledgments

The author would like to thank the Office of Naval Research for financial support under the direction of Dr. Steve McElvaney. Many thanks to Mr. Steve Enzinger, Mr. Don Bunker, and the rest of the USNA Hydromechanics Lab staff for providing technical support.

Nomenclature

B = smooth wall log-law intercept=5.0
C_F = overall frictional resistance coefficient $=(F_D)/(1/2\rho U_e^2 S)$
c_f = local frictional resistance coefficient=$(\tau_o)/(\frac{1}{2}\rho U_e^2)$
F_D = drag force
k = arbitrary measure of roughness height
L = plate length
N = number of samples in surface profile
Re_{δ^*} = displacement thickness Reynolds number=$U_e\delta^*/\nu$
Re_L = Reynolds number based on plate length=U_eL/ν
R_a = centerline average roughness height=$1/N\Sigma_{i=1}^{N}|y_i|$
R_q = root mean square roughness height=$\sqrt{1/N\Sigma_{i=1}^{N}y_i^2}$
R_t = maximum peak to through height=$y_{\max}-y_{\min}$
S = wetted surface area
U = mean velocity in the x direction
U_e = freestream velocity relative to surface
U_τ = friction velocity=$\sqrt{\tau_o/\rho}$
ΔU^+ = roughness function
x = streamwise distance from plate leading edge
y = normal distance from the boundary measured from roughness centerline
δ = boundary layer thickness
δ^* = displacement thickness=$\int_0^\delta(1-U/U_e)dy$
κ = von Karman constant=0.41
ν = kinematic viscosity of the fluid
ρ = density of the fluid
τ_o = wall shear stress

superscript

$+$ = inner variable (normalized with U_τ or U_τ/ν)

subscript

min = minimum value
max = maximum value
R = rough surface
S = smooth surface

References

[1] Kempf, G., 1937, ''On the Effect of Roughness on the Resistance of Ships,'' Trans. Institution of Naval Architects **79**, pp. 109–119.
[2] Benson, J. M., Ebert, J. W., and Beery, T. D., 1938, ''Investigation in the NACA Tank of the Effect of Immersion in Salt Water on the Resistance of Plates Coated With Different Shipbottom Paints,'' N.A.C.A. Memorandum Report C&R C-S19-1(3).
[3] Denny, M. E., 1951, ''B.S.R.A. Resistance Experiments on the Lucy Ashton: Part I—Full-Scale Measurements,'' Trans. Institution of Naval Architects **93**, pp. 40–57.
[4] Lewthwaite, J. C., Molland, A. F., and Thomas, K. W., 1985, ''An Investigation Into the Variation of Ship Skin Frictional Resistance With Fouling,'' Trans. Royal Institute of Naval Architect., **127**, pp. 269–284.
[5] Watanabe, S., Nagamatsu, N., Yokoo, K., and Kawakami, Y., 1969, ''The Augmentation in Frictional Resistance Due to Slime,'' J. Kansai Society of Naval Architects, **131**, pp. 45–51.
[6] Leer-Andersen, M., and Larsson, L., 2003, ''An Experimental/Numerical Approach for Evaluating Skin Friction on Full-Scale Ships With Surface Roughness,'' J. Marine Sci. Technol., **8**, pp. 26–36.
[7] Townsin, R. L., 2003, ''The Ship Hull Fouling Penalty,'' Biofouling, **19**(**Supplement**), pp. 9–16.
[8] Swain, G., 1998, ''Biofouling Control: A Critical Component of Drag Reduction,'' *Proceedings of the International Symposium on Seawater Drag Reduction*, Newport, RI, pp. 155–161.
[9] Champ, M. A., 2003, ''Economic and Environmental Impacts on Port and Harbors From the Convention to Ban Harmful Marine Anti-Fouling Systems,'' Mar. Pollution Bull., **46**, pp. 935–940.
[10] Swain, G. W., and Schultz, M. P., 1996, ''The Testing and Evaluation of Non-Toxic Antifouling Coatings,'' Biofouling, **10**, pp. 187–197.
[11] Candries, M., Atlar, M., and Anderson, C. D., 2000, ''Considering the Use of Alternative Antifoulings: the Advantages of Foul-Release Systems,'' *Proceedings ENSUS 2000*, Newcastle, UK, pp. 88–95.
[12] Brady, R. F., and Singer, I. L., 2000, ''Mechanical Factors Favoring Release From Fouling Release Coatings,'' Biofouling, **15**, pp. 73–81.
[13] Schultz, M. P., Finlay, J. A., Callow, M. E., and Callow, J. A., 2003, ''Three Models to Relate Detachment of Low Form Fouling at Laboratory and Ship Scale,'' Biofouling, **19**(Supplement), pp. 17–26.
[14] Swain, G. W., Nelson, W. G., and Preedeekanit, S., 1998, ''The Influence of Biofouling and Biotic Disturbance on the Development of Fouling Communities on Non-Toxic Surfaces,'' Biofouling, **12**, pp. 257–269.
[15] Kavanagh, C. J., Schultz, M. P., Swain, G. W., Stein, J., Truby, K., and Darkangelo Wood, C., 2001, ''Variation in Adhesion Strength of Balanus Eburneus, Crassotrea Virginica and Hydroides Dianthus to Fouling-Release Coatings,'' Biofouling, **17**, pp. 155–167.
[16] Kovach, B. S., and Swain, G. W., 1998, ''A Boat-Mounted Foil to Measure the Drag Properties of Antifouling Coatings Applied to Static Immersion Panels,'' *Proceedings of the International Symposium on Seawater Drag Reduction*, Newport, RI, pp. 169–173.
[17] Lackenby, H., 1962, ''Resistance of Ships, With Special Reference to Skin Friction and Hull Surface Condition,'' *Proceedings of the Institution of Mechanical Engineers*, **176**, pp. 981–1014.
[18] Musker, A. J., 1980–1981, ''Universal Roughness Functions for Naturally-Occurring Surfaces,'' Trans. Can. Soc. Mech. Eng., **1**, pp. 1–6.
[19] Townsin, R. L., Byrne, D., Svensen, T. E., and Milne, A., 1981, ''Estimating the Technical and Economic Penalties of Hull and Propeller Roughness,'' Trans. SNAME, **89**, pp. 295–318.
[20] Granville, P. S., 1987, ''Three Indirect Methods for the Drag Characterization of Arbitrarily Rough Surfaces on Flat Plates,'' J. Ship Res., **31**, pp. 70–77.
[21] Medhurst, J. S., 1989, ''The Systematic Measurement and Correlation of the Frictional Resistance and Topography of Ship Hull Coatings, With Particular Reference to Ablative Antifoulings,'' Ph.D. Thesis, University of Newcastle-upon-Tyne, Newcastle, UK.
[22] Grigson, C. W. B., 1992, ''Drag Losses of New Ships Caused by Hull Finish,'' J. Ship Res., **36**, pp. 182–196.
[23] Anon, 1952, *Marine Fouling and Its Prevention*, Woods Hole Oceanographic Institution.
[24] McEntee, W., 1915, ''Variation of Frictional Resistance of Ships With Condition of Wetted Surface,'' Trans. SNAME, **24**, pp. 37–42.
[25] Picologlou, B. F., Zelver, N., and Characklis, W. G., 1980, ''Biofilm Growth and Hydraulic Performance,'' J. Hydraul. Div., Am. Soc. Civ. Eng., **HY5**, pp. 733–746.
[26] Haslbeck, E. G., and Bohlander, G., 1992, ''Microbial Biofilm Effects on Drag—Lab and Field,'' *Proceedings 1992 SNAME Ship Production Symposium*.
[27] Schultz, M. P., and Swain, G. W., 1999, ''The Effect of Biofilms on Turbulent Boundary Layers,'' ASME J. Fluids Eng., **121**, pp. 733–746.
[28] Schultz, M. P., 2000, ''Turbulent Boundary Layers on Surfaces Covered With Filamentous Algae,'' ASME J. Fluids Eng., **122**, pp. 357–363.
[29] Clauser, F. H., 1954, ''Turbulent Boundary Layers in Adverse Pressure Gradients,'' J. Aeromaut. Sci. , **21**, pp. 91–108.
[30] Hama, F. R., 1954, ''Boundary-Layer Characteristics for Rough and Smooth Surfaces,'' Trans. SNAME, **62**, pp. 333–351.
[31] Krogstad, P. Å., and Antonia, R. A., 1999, ''Surface Roughness Effects in Turbulent Boundary Layers,'' Exp. Fluids, **27**, pp. 450–460.
[32] Schultz, M. P., and Flack, K. A., 2003, ''Turbulent Boundary Layers Over Surfaces Smoothed by Sanding,'' ASME J. Fluids Eng., **125**, pp. 863–870.
[33] Schultz, M. P., and Myers, A., 2003, ''Comparison of Three Roughness Function Determination Methods,'' Exp. Fluids, **35**, pp. 372–379.
[34] Granville, P. S., 1958, ''The Frictional Resistance and Turbulent Boundary Layer of Rough Surfaces,'' J. Ship Res., **2**, pp. 52–74.
[35] Schultz, M. P., 2002, ''The Relationship Between Frictional Resistance and Roughness for Surfaces Smoothed by Sanding,'' ASME J. Fluids Eng., **124**, pp. 492–499.

[36] ASTM D3623, 1994, ''Standard Test Method for Testing Antifouling Panels in Shallow Submergence,'' Vol. 6.02.
[37] Moffat, R. J., 1988, ''Describing the Uncertainties in Experimental Results,'' Exp. Therm. Fluid Sci., **1**, pp. 3–17.
[38] Coleman, H. W., and Steele, W. G., 1995, ''Engineering Application of Experimental Uncertainty Analysis,'' AIAA J., **33**(10), pp. 1888–1896.
[39] Schoenherr, K. E., 1932, ''Resistances of Flat Surfaces Moving Through a Fluid,'' Trans. SNAME, **40**, pp. 279–313.
[40] Candries, M., Atlar, M., Mesbahi, E., and Pazouki, K., 2003, ''The Measurement of the Drag Characteristics of Tin-Free Self-Polishing Co-Polymers and Fouling Release Coatings Using a Rotor Apparatus,'' Biofouling, **19**(Supplement), pp. 27–36.
[41] Schlichting, H., 1979, *Boundary-Layer Theory*, 7th ed., McGraw-Hill, New York.
[42] Nikuradse, J., 1933, ''Laws of Flow in Rough Pipes,'' *NACA Technical Memorandum 1292*.
[43] Bradshaw, P., 2000, ''A Note on ''Critical Roughness Height'' and ''Transitional Roughness'','' Phys. Fluids, **12**, pp. 1611–1614.